Supplementary Information (SI) for Sustainable Energy & Fuels.

Supporting Information

Efficient Cascade Conversion of Glucose to Levulinic Acid using Dual-Functional UiO-66 Catalyst

Sininat Boonmark,[a] Panyapat Ponchai,[a] Kanyaporn Adpakpang,[a] Taya Saothayanun,[a]

*Yollada Inchongkol,[a] Natchaya Phongsuk[a] and Sareeya Bureekaew[*a]*

[a] School of Energy Science and Engineering, Vidyasirimedhi Institute of Science and Technology, 555

Moo 1 Payupnai, Wangchan, Rayong 21210, Thailand

**E-mail*: Sareeya.b@vistec.ac.th

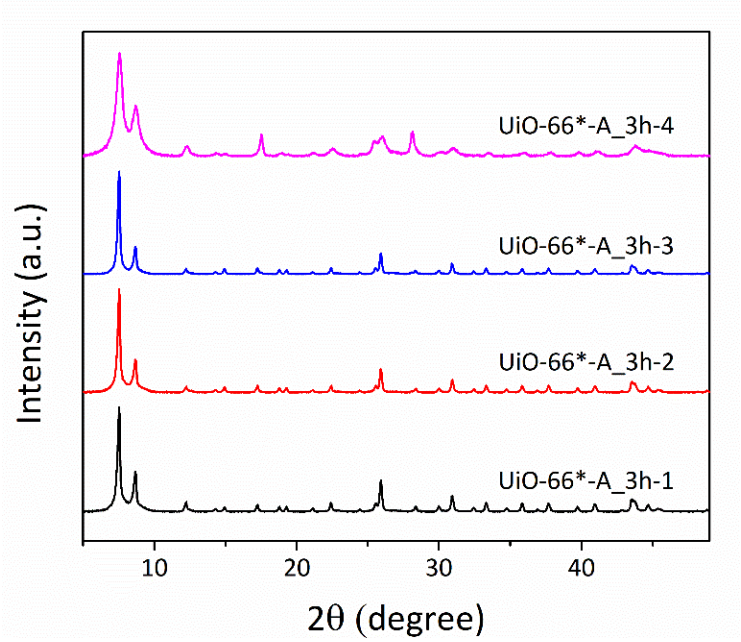

Figure S1. Powder X-ray diffraction (PXRD) patterns of the UiO-66*-A after acid treatment. The crystallinity of UiO-66*-A remained stable up to the 3rd cycle.

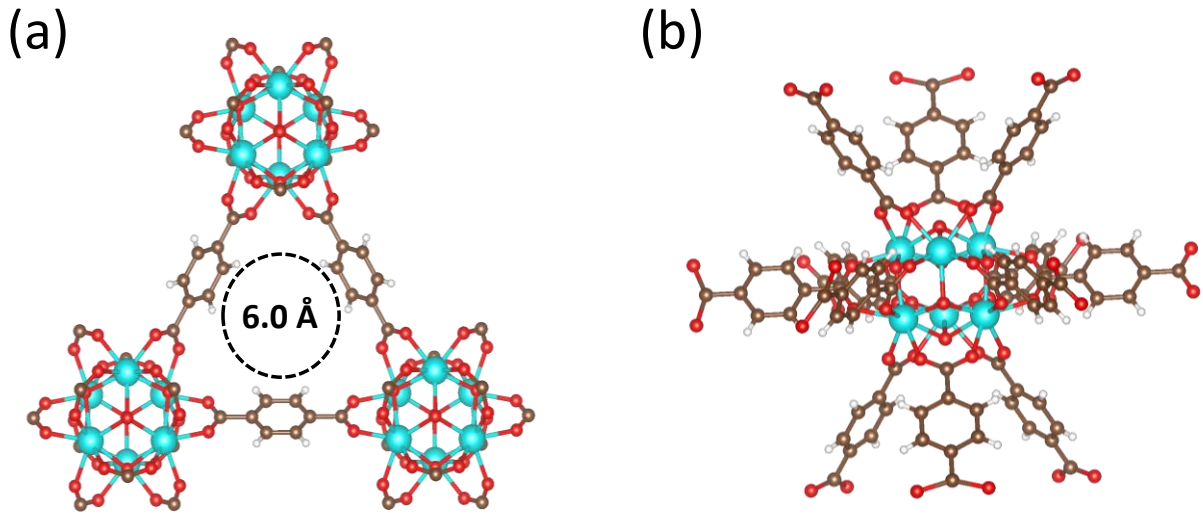

Figure S2. Structural illustration of UiO-66 presenting: (a) a pore window with the size of *c.a.* 6.0 Å, and (b) building unit of $Zr_6O_4(OH)_4(BDC)_{12}$. (Color: Zr, blue; O, red; C, brown; H, white).

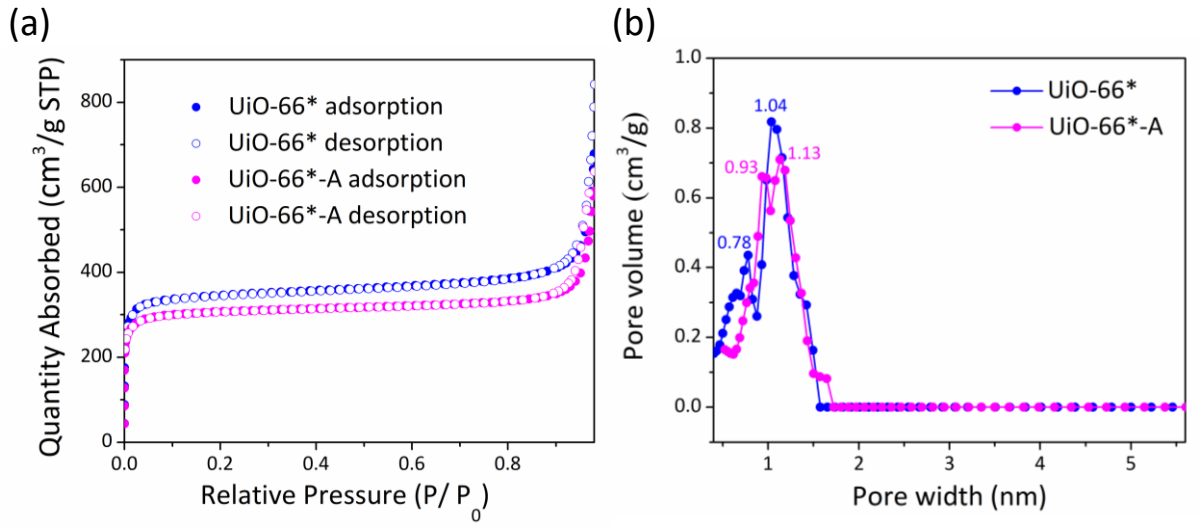

Figure S3. (a) N_2 sorption isotherms and (b) pore size distribution of the UiO-66* and UiO-66*-A measured at 77 K.

Table S1. Summary surface areas and pore volumes of UiO-66* and UiO-66*-A calculated from N_2 sorption isotherms using Brunauer–Emmett–Teller (BET) and t-plot analysis.

Sample	Specific surface area ($m^2 g^{-1}$)	Total pore volume ($cm^3 g^{-1}$)
UiO-66*	1382.6	0.4746
UiO-66*-A	1234.3	0.4344

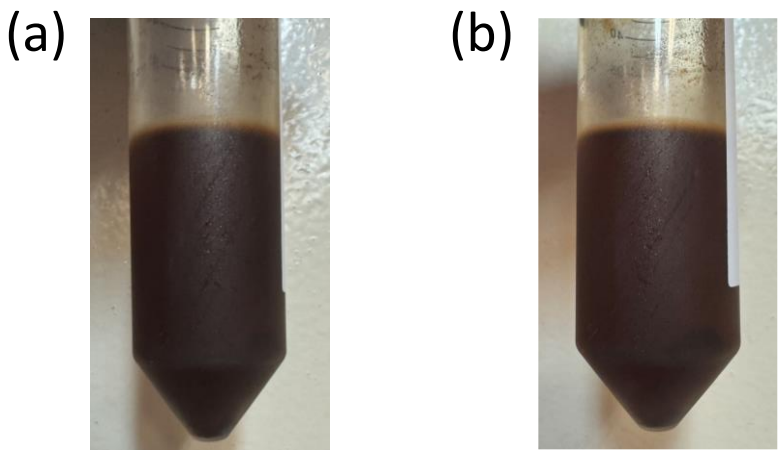

Figure S4. Photographs of an absence of catalyst (a) without and (b) with NaCl salt after hydrothermal reactions at 190 °C for 6 h, respectively.

Table S2. Conversions and yields for the catalytic conversion of glucose into LEV on UiO-66*-A catalyst over 6 h at various reaction temperatures.

Reaction temperature (°C)	Glucose conversion (%)	Fructose (mol)	LEV (mol)	5-HMF (mol)	LA (mol)
150	64.66 ± 0.52	0.05 ± 0.00	0.01 ± 0.00	0.09 ± 0.00	0.04 ± 0.00
170	83.58 ± 0.13	0.02 ± 0.00	0.19 ± 0.01	0.07 ± 0.00	0.06 ± 0.00
190	>99.00	*n.d.* [a]	0.58 ± 0.01	0.06 ± 0.00	0.05 ± 0.01

[a]n.d.= not detected

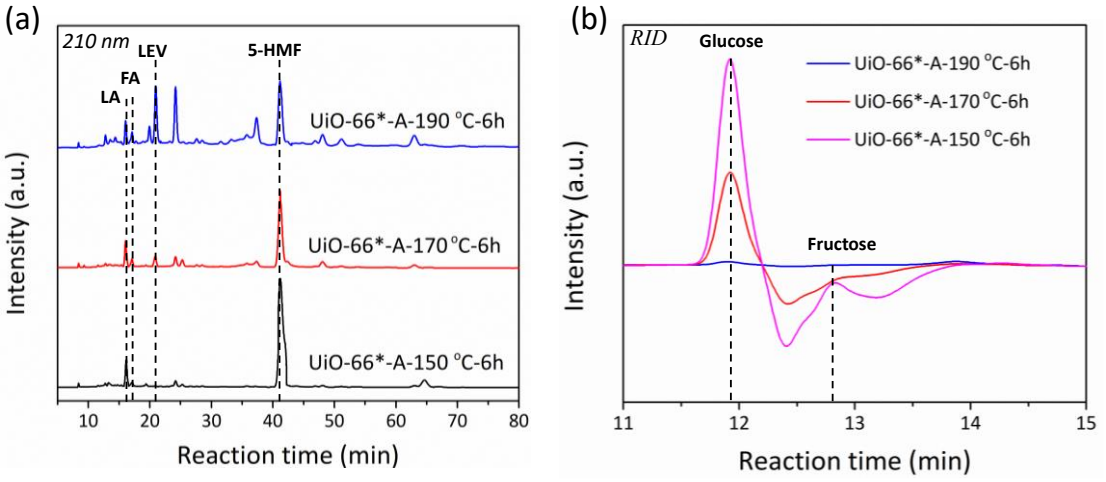

Figure S5. HPLC chromatograms from (a) UV (210 nm) and (b) RID detectors of the supernatants from the reactions employing UiO-66*-A as the catalyst at various temperatures for 6 h.

: This figure illustrates HPLC chromatograms obtained from UV (210 nm) and RID detectors of the supernatants. The chromatograms from UV detector quantify the resulting LEV, HMF, and LA from the reaction, while the results from the RID detector provide information on glucose and fructose. At a low reaction temperature of 150 °C, a prominent fructose peak is observed (0.05 mol, Table S2). As the reaction temperature increases to 170 and 190 °C, only trace amounts of fructose can be observed. These results indicate that the UiO-66*-A catalyst efficiently converts glucose to fructose before dehydration and hydrolysis processes, which ultimately lead to LEV production.

Table S3. Conversions and yields of the catalytic performance of UiO-66*-A for 190 °C at various reaction times.

Reaction time (h)	Glucose conversion (%)	LEV (mol)	5-HMF (mol)	LA (mol)
2	72.71 ± 0.59	0.28 ± 0.00	0.04 ± 0.00	0.04 ± 0.01
4	84.67 ± 0.57	0.41 ± 0.01	0.09 ± 0.01	0.08 ± 0.01
6	>99.00	0.58 ± 0.00	0.06 ± 0.00	0.05 ± 0.01
9	>99.00	0.37 ± 0.00	0.01 ± 0.00	0.03 ± 0.01

Table S4. Conversions and yields for catalytic conversion of glucose into LEV at the various amount of UiO-66*-A catalyst at 190 °C for 6 h.

Amount of catalyst (g)	Glucose conversion (%)	LEV (mol)	5-HMF (mol)	LA (mol)
0.10	96.98 ± 0.14	0.46 ± 0.01	0.05 ± 0.00	0.04 ± 0.00
0.20	>99.00	0.58 ± 0.01	0.06 ± 0.00	0.05 ± 0.01
0.30	>99.00	0.60 ± 0.01	0.04 ± 0.00	0.05 ± 0.00

Table S5. Conversions and yields for catalytic conversion of glucose into LEV at the various amount of NaCl salt on UiO-66*-A catalyst at 190 °C for 6 h.

Catalyst	[a]NaCl salt (w/w)	Glucose conversion (%)	LEV (mol)	5-HMF (mol)	LA (mol)
UiO-66*-A	none	>99.00	0.58 ± 0.01	0.06 ± 0.00	0.05 ± 0.01
UiO-66*-A	0.5	>99.00	0.60 ± 0.01	0.01 ± 0.00	0.04 ± 0.01
UiO-66*-A	1	>99.00	0.75 ± 0.01	0.02 ± 0.01	0.03 ± 0.01
UiO-66*-A	2	>99.00	0.83 ± 0.01	0.02 ± 0.00	0.02 ± 0.01
UiO-66*-A	3	>99.00	0.84 ± 0.00	0.02 ± 0.00	0.02 ± 0.02

[a]NaCl to glucose ratio (w/w).

(a)

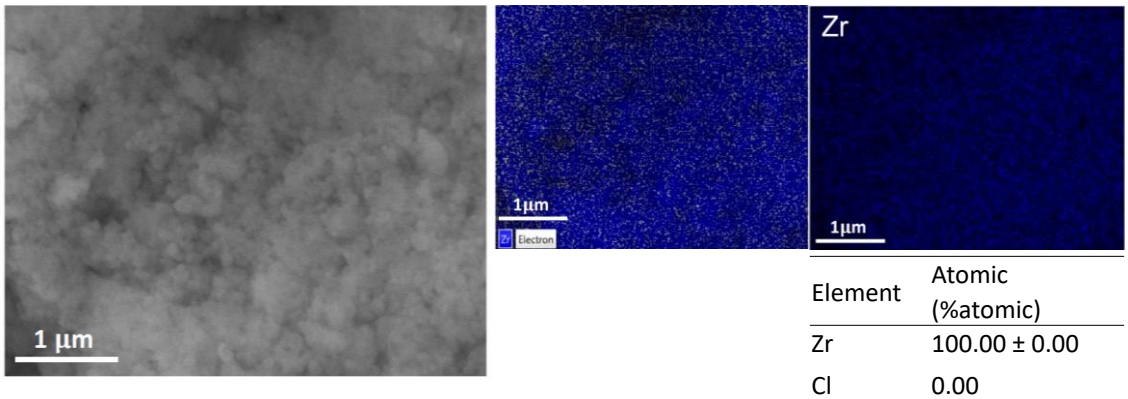

Element	Atomic (%atomic)
Zr	100.00 ± 0.00
Cl	0.00

(b)

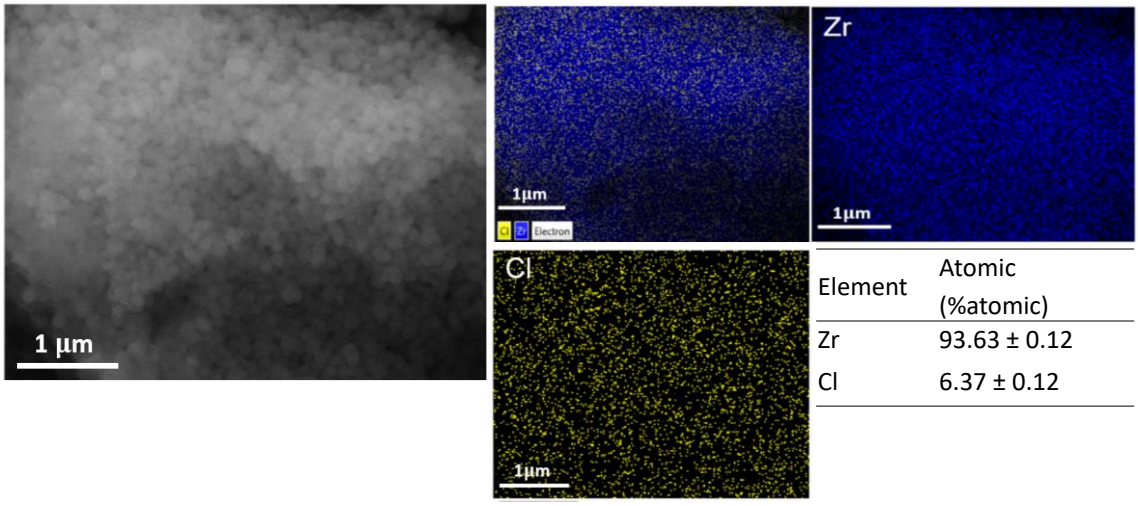

Element	Atomic (%atomic)
Zr	93.63 ± 0.12
Cl	6.37 ± 0.12

Figure S6. Scanning electron microscopy-energy dispersive X-ray spectroscopy (SEM-EDS) mapping of (a) UiO-66* and (b) UiO-66*-A.

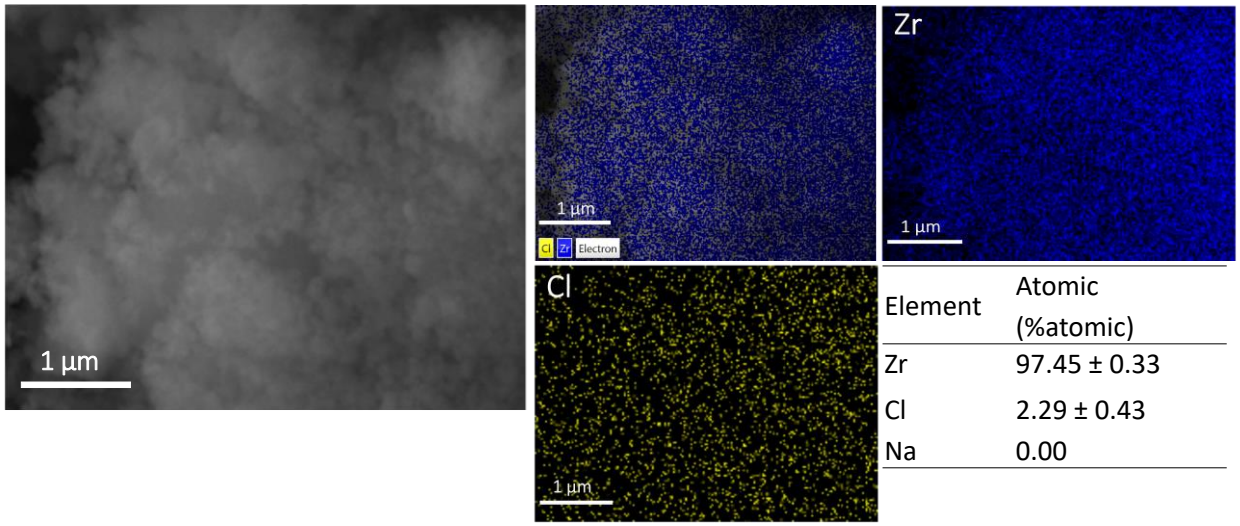

Element	Atomic (%atomic)
Zr	97.45 ± 0.33
Cl	2.29 ± 0.43
Na	0.00

Figure S7. SEM-EDS mapping of UiO-66*-A after the glucose conversion reaction at 190 °C for 6 h.

: SEM-EDS analysis confirmed the absence of Na in the used catalyst, likely due to the acidic final solution (pH 2-3), which promotes the formation of –COOH groups instead of –COONa.

Table S6. Comparisons of catalytic performance of different MOF catalysts investigated for the conversion of glucose into HMF and LEV under various conditions.

Entry	Catalyst	Reactant	Conversion (%)	Yield (mol)	Solvent	Condition	Ref.
1	PTA/MIL-101	fructose	82.00%	0.63mol HMF	DMSO	130 °C, 30 m	1
2	MIL-101(Cr)-SO_3H	fructose	> 99.00%	0.90mol HMF	DMSO	120 °C, 1 h	2
3	Fe/MIL-101 (Cr)	glucose	91.50%	0.56mol HMF	DMSO/H_2O	170 °C, 2 h	3
4	PO_4/NU-1000	glucose	> 99.00%	0.64mol HMF	H_2O/2PrOH	140 °C, 7 h	4
5	MIL-100(Fe)/ Lys-PM_2	glucose	98.70%	0.58mol LEV	H_2O	150 °C, 9 h	5
6	UiO-66-NH-R-SO_3H	glucose	> 99.00%	0.72mol LEV	H_2O	170 °C, 24 h	6
7	UiO-66*-A	glucose	> 99.00%	0.83mol LEV	H_2O	190 °C, 6 h	this work

: Several MOFs with Lewis and Bronsted acid attributes have been proposed for catalytic conversion of C6 sugars (*e.g.,* glucose and fructose) to 5-HMF (entries 1-4). Only a few MOF catalysts effectively convert glucose to LEV. Examples include MIL-100(Fe) loaded with an insoluble lysine-functionalized phosphotungstic acid (entry 5) and UiO-66-NH-R-SO_3H (entry 6) achieving a yield of 0.58 and 0.72 LEV, respectively. In this study (entry 7), we successfully modified UiO-66 through the post-synthetic treatment method. The resulting defect-engineered UiO-66 exhibiting both Lewis and Bronsted acid characteristics enables to catalyze a multistep reaction, achieving LEV yield of 0.83 mol/mol of glucose and complete glucose conversion under hydrothermal condition in the presence of NaCl.

Table S7. Carbon content (%) of the UiO-66*-A catalyst before and after the glucose conversion reaction at 190 °C for 6 h, as determined by CHNS elemental analysis.

Entry	Sample	Carbon (%)
1	UiO-66*-A	22.52 ± 0.10
2	UiO-66*-A _1st	34.84 ± 0.20
3	UiO-66*-A _2nd	38.26 ± 0.36
4	UiO-66*-A _3rd	40.41 ± 0.26

: The carbon content in the spent catalysts increases significantly during recycling, confirming the accumulation of additional carbonaceous substances within the framework. This accumulation hinders the diffusion of glucose into the framework, preventing it from accessing the active sites and ultimately leading to a decline in catalytic performance in subsequent runs. It is worth noting that regeneration of the spent catalyst was performed by washing it with hot methanol.

Table S8. Catalytic performance at different stirring speeds (300 and 400 rpm) under reaction conditions of 190 °C.

Reaction time (h)	Stirring speed (rpm)	Glucose conversion (%)	LEV (mol)	5-HMF (mol)	LA (mol)
4	300	84.67 ± 0.57	0.41 ± 0.01	0.09 ± 0.01	0.08 ± 0.01
	400	84.73 ± 0.73	0.40 ± 0.00	0.10 ± 0.00	0.08 ± 0.01
6	300	>99.00	0.58 ± 0.00	0.06 ± 0.00	0.05 ± 0.01
	400	>99.00	0.59 ± 0.00	0.06 ± 0.01	0.05 ± 0.01

: The catalytic performance at stirring speeds of 300 and 400 rpm was comparable. This confirms that the reaction kinetics are unaffected by stirring speed.

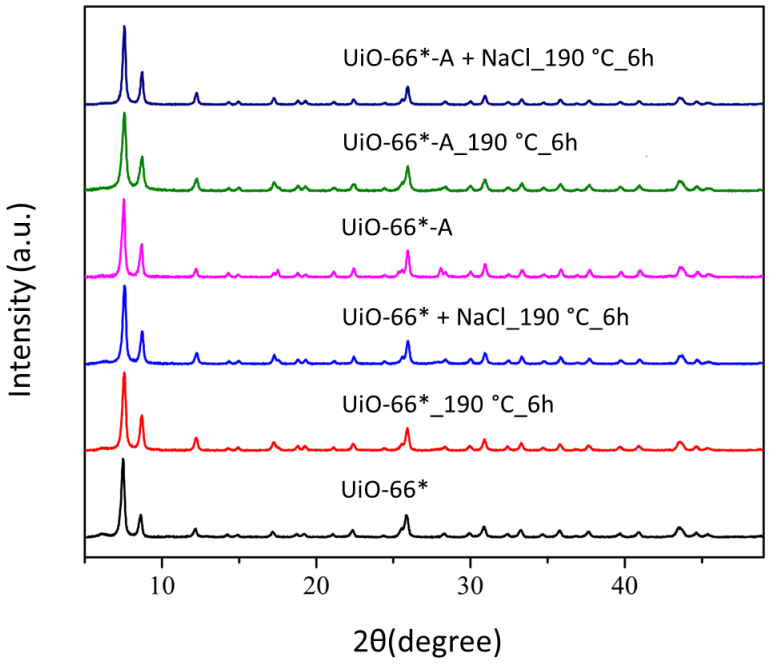

Figure S8. PXRD patterns of the UiO-66* and UiO-66*-A before and after the glucose conversion reaction with and without NaCl at 190 °C for 6 h, respectively.

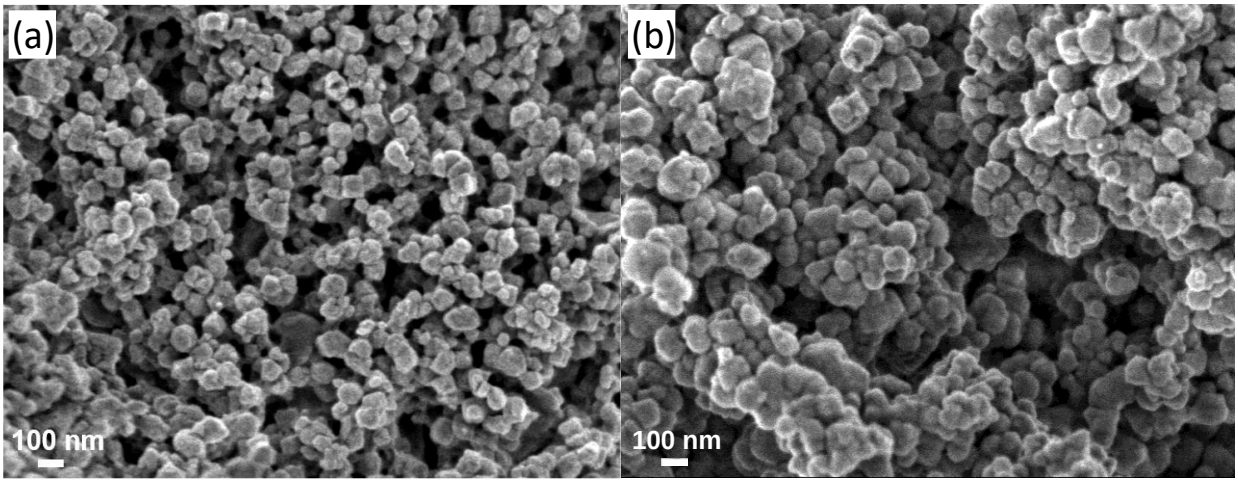

Figure S9. Scanning electron microscopic (SEM) images of (a) UiO-66*-A before and (b) UiO-66*-A after the reaction at 190 °C 6 h, respectively.

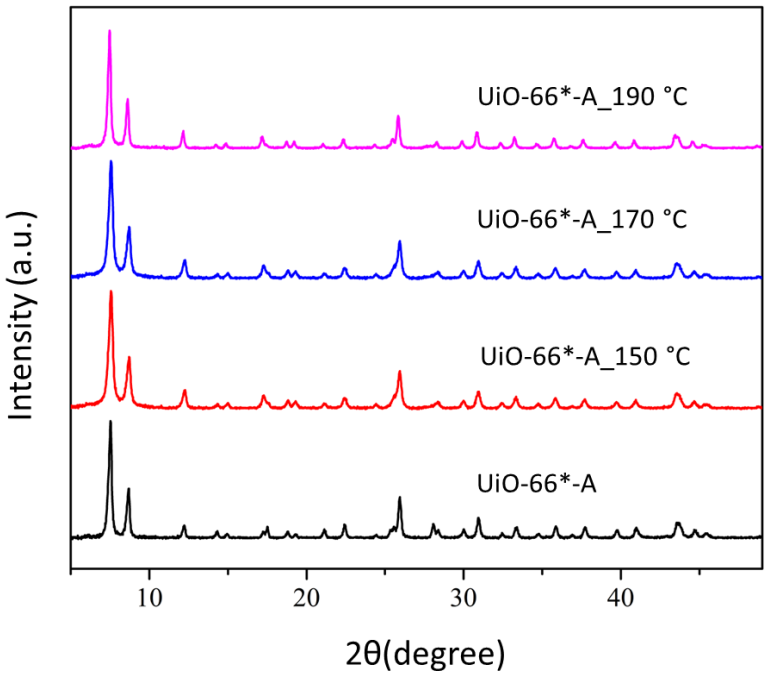

Figure S10. PXRD patterns of the UiO-66*-A before and after the reaction at various temperatures for 6 h.

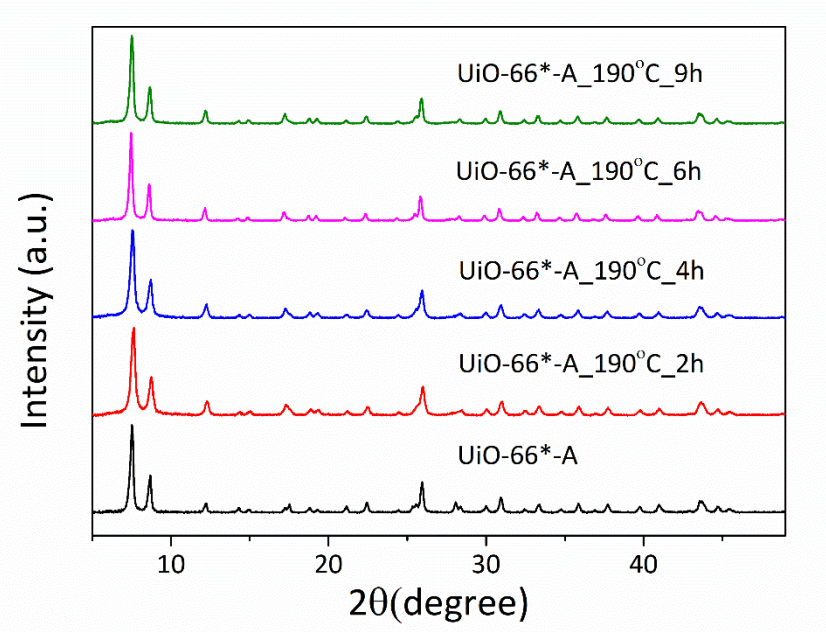

Figure S11. PXRD patterns of the UiO-66*-A before and after the reactions at 190 °C for various reaction times.

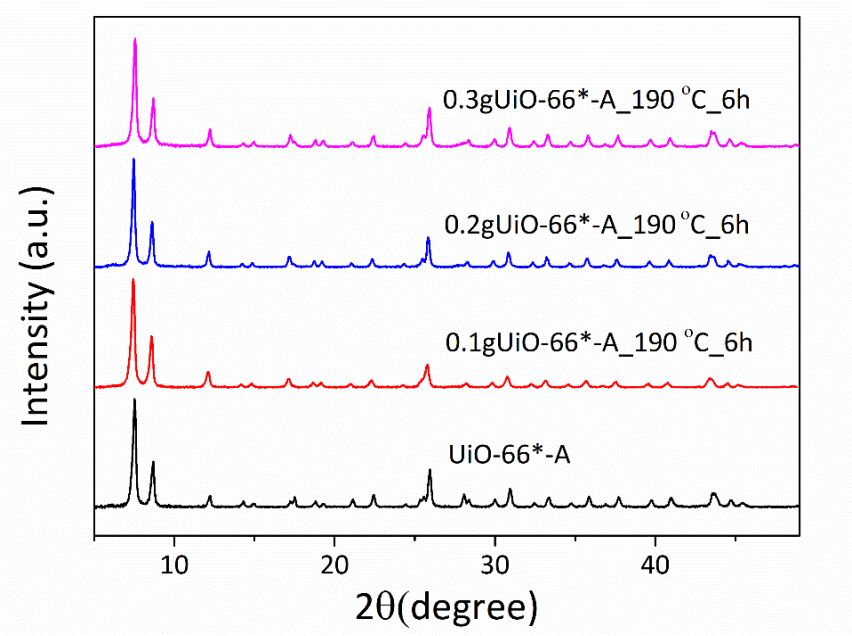

Figure S12. PXRD patterns of the UiO-66*-A before and after the reaction at 190 °C for 6 h at various amount of catalyst.

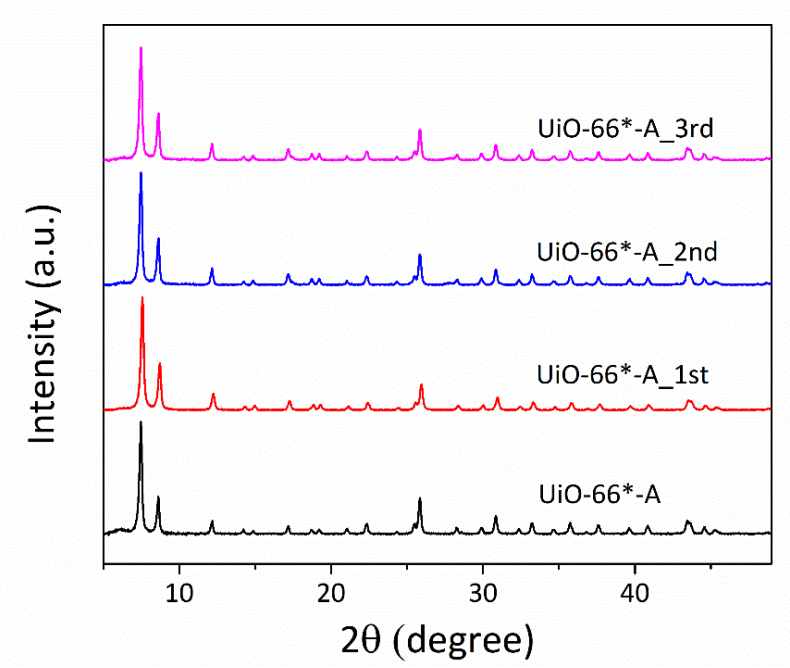

Figure S13. PXRD patterns of the UiO-66*-A before and after the glucose conversion reaction at 190 °C for 6 h over three consecutive cycles.

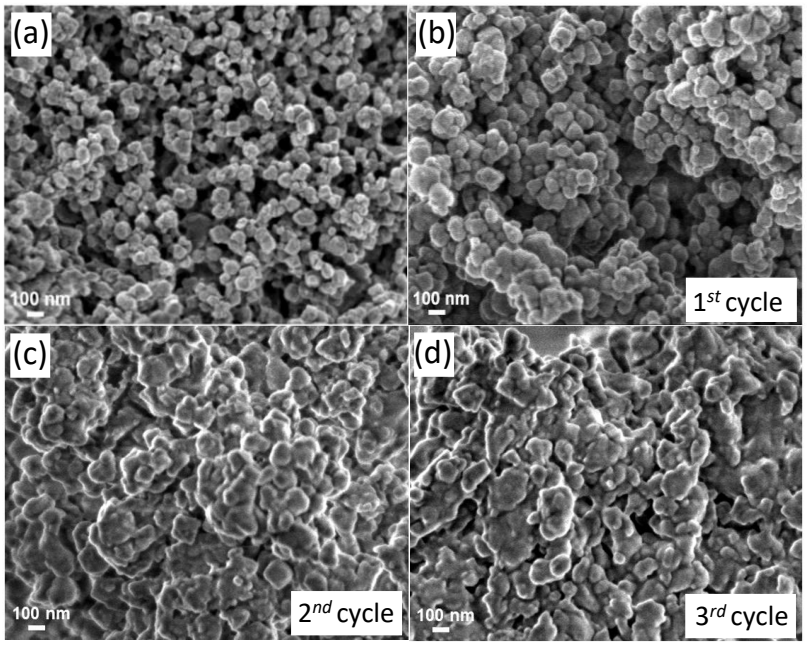

Figure S14. SEM images of the UiO-66*-A before and after the glucose conversion reaction at 190 °C for 6 h over 3 cycles of test.

REFERENCES

1 Y. Zhang, V. Degirmenci, C. Li and E. J. M. Hensen, Phosphotungstic Acid Encapsulated in Metal-Organic Framework as Catalysts for Carbohydrate Dehydration to 5-Hydroxymethylfurfural, *ChemSusChem,* 2011, **4**, 59-64.

2 J. Chen, K. Li, L. Chen, R. Liu, X. Huang and D. Ye, Conversion of Fructose into 5-Hydroxymethylfurfural Catalyzed by Recyclable Sulfonic Acid-functionalized Metal–Organic Frameworks, *Green Chem.,* 2014, **16**, 2490-2499.

3 C. Lu, Y. Zhou, L. Li, H. Chen and L. Yan, Conversion of Glucose into 5-Hydroxymethylfurfural Catalyzed by Cr-and Fe-containing Mixed-Metal Metal–Organic Frameworks, *Fuel,* 2023, **333**, 126415.

4 M. Yabushita, P. Li, T. Islamoglu, H. Kobayashi, A. Fukuoka, O. K. Farha and A. Katz, Selective Metal-Organic Framework Catalysis of Glucose to 5-Hydroxymethylfurfural Using Phosphate-Modified NU-1000, *Ind. Eng. Chem. Res.,* 2017, **56**, 7141-7148.

5 H. Qu, B. Liu, G. Gao, Y. Ma, Y. Zhou, H. Zhou, L. Li, Y. Li and S. Liu, Metal-Organic Framework Containing Brønsted Acidity and Lewis Acidity for Efficient Conversion Glucose to Levulinic Acid, *Fuel Process. Technol*., 2019, **193**, 1-6.

6 B. W. Lee, J. Y. Seo, K. Jeong, J. Choi, K. Y. Cho, S. Cho, K.-Y. Baek, Efficient Production of Levulinic Acid using Metal-Organic Framework Catalyst: Role of Brønsted Acid and Flexibility, *Chem. Eng. Sci.,* 2022, **444**, 136566.